SSRG International Journal of Electrical and Electronics Engineering
ISSN: 2348-8379/ https://doi.org/10.14445/23488379/IJEEE-V10I9P116

Volume 10 Issue 9, 167-180, September 2023

Original Article

Design and Simulation of Conformal Array Antennas for Avionics Applications

Pushpa B R[1], Pushpa P V[2], Devaraju Ramakrishna[3]

[1,2]*Department of Electronics and Communication Engineering, Dayananda Sagar University, Karnataka, India.*
[3]*Department of Electronics and Telecommunication Engineering, Dayananda Sagar College of Engineering, Karnataka, India.*

[1]*Corresponding Author : pushpa-tce@dayanandasagar.edu*

Received: 22 July 2023 Revised: 25 August 2023 Accepted: 17 September 2023 Published: 30 September 2023

Abstract *- Conformal array antennas have become an integral part of avionics and many other diversified applications because of their capacity to provide increased gain, conformity to the shape of the mount on which they are placed and durability. The present paper presents a novel approach plus meticulous design, simulation and comparison of results obtained for two configurations of microstrip patch antennas and arrays fed with an inset feed technique for avionics applications in 5G technology. The inset feed technique optimizes the impedance matching of the antennas. The resonating frequencies of 3.6 GHz and 3.4 GHz are selected for uplink and downlink, respectively, from the n78 band of 5G communication in India. The methodology used for designing single antenna elements is extended to a 1x2 array. The parameters used for assessing simulation results using CST (Computer Simulation Technology) Studio Suite, version 2017.0224 software, are Antenna Bandwidth (Return Loss) plots, VSWR plots, impedance plots, and gain plots of radiation patterns in both 2D and 3D. The simulated results show a considerable increase in gain, SWR and return loss for a 1x2 array compared to a single radiating patch. Antennas and arrays thus designed find applications invariably in aircraft, air traffic control management, drones and navigation systems as point-to-point communication links.*

Keywords *- Conformal arrays, Downlink, n78 band, Uplink, 5G communications.*

1. Introduction

Conformal antennas conform to a particular shape, which can be a part of an aircraft, vehicle or some other mechanical part of a machine. Conformal antennas are lightweight structures for radio frequency applications. They suit curved geometry and provide nearly 360° coverage with significantly fewer limitations.

The purpose of conformal antennas is to mingle with the surface mount thoroughly and not cause extra drag or aircraft fuselage. If the designed antenna can be less disturbing and less visible to the human eye, it can be used in aircraft and military applications. Modern requirement for the conformal antenna is that it should not have stealth (that is, it should not glare back or radiate back the signal from an enemy aircraft or missile) properties.

Types of conformal arrays are circular, cylindrical, conical arrays and other shapes with rotational symmetry. Conformal antennas are widely employed in avionics equipment like rockets, drones, high-velocity flying machines, aircraft, etc. Another advantage of conformal antennas is that it doesn't require the radome installation, thereby eliminating the losses caused by minor lobes of the radiation pattern. So far, conformal arrays have been designed and developed mainly for military and defence purposes. They were seldom employed for commercial applications because of the complexity of design and the high costs involved in their fabrication and integration into the equipment or radome structure. This work presents a novel approach to design and simulate the microstrip patches that give the platform for conformal array design targeted for 5G communications, which is state-of-the-art technology. 5G bands are the range of frequencies used by 5G cellular networks. The frequencies and band designations of 5G, as followed in India, are summarized in Table 1.

Table 1. 5G bands in India

Frequency (MHz)	5G Bands
3300-3800	n78
3300-4200	n77
4400-5000	n79
26 GHz (24.25-27.5 GHz)	n258

5G networks employ different sets of frequencies for data transmission and internet facilities. 5G communications connect people and things worldwide with a common platform for exchanging information at very high speeds that could have never been imagined before. 5G bands in India are divided mainly into low-frequency, mid-frequency and high band-mm Wave.

The frequency range from 3300 MHz to 3800 MHz is the n78 band. The n78 comes under the mid-band category and is accessible throughout the world. Its cost-effectiveness and capacity to deliver data speeds up to 1Gbps make it most attractive to telecom service providers.

However, it may not be as fast as the mm-Wave 5G technology. N78 (3500 MHz) is commonly designated as 3.5 GHz 5G or C-band 5G. The selected frequency for uplink is 3.6 GHz, and that for downlink is 3.4 GHz, both of which fall in the n78 band of 5G.

2. Design

The design of the antenna structure is divided into two broad categories. The former is the design of a single microstrip patch antenna with a feed network for radiating at two different frequencies for uplink and downlink separately.

The latter is the design of a 1x2 array with two elements, a power divider and a feed network for the same uplink and downlink frequencies. The essential parameters considered for design are listed below.

1. Frequency of operation or resonant frequency: 3.6 GHz for the uplink and 3.4 GHz for the downlink.
2. Polarization: Linear
3. Impedance Matching: 50Ω according to Indian standards for matching the impedance of the microstrip patch to the feeding transmission line.
4. Array configuration: Conformal
5. Substrate material: FR-4 with dielectric constant 4.3
6. Feed Method: Inset feed to achieve the best impedance matching.
7. Array dimensions: Includes array geometry, configuration and interelement spacing.

The necessary design equations for a single patch and array are as follows.

2.1. Single Patch Design

The formula gives the width of the rectangular patch,

$$w = \frac{c}{2f_0\sqrt{(\frac{\varepsilon_r+1}{2})}} \quad (1)$$

Where 'ε_r' is the dielectric constant of the material used for the substrate, 'c' is the speed of light in vacuum with numerical value $3x10^8$ ms^{-1} and 'f_0' is the resonant frequency of uplink or downlink. Here, the dielectric material used is FR-4, with a dielectric constant 4.3. The length and width of the ground plane, which is equal to the height and width of the substrate, are calculated by the equations,

$$L_g = 6h + L \quad (2)$$

$$W_g = 6h + W \quad (3)$$

2.2. 1x2 Array Design

An important parameter called effective refractive index must be calculated for the microstrip patch array. When the radiations from the patch towards the ground pass through the air, they split and pass through the dielectric, also known as fringing. This needs to be avoided. Since air and dielectrics have different refractive indices, the practical value of the dielectric constant, called the effective refractive index, must be found. It is given by,

$$\varepsilon_{eff} = \frac{\varepsilon_r+1}{2} + \frac{\varepsilon_r-1}{2}\left[\frac{1}{1+12(^h/_w)}\right] \quad (4)$$

Where (w/h)>1 and 'h' is the height of the substrate. ε_{eff} must be calculated for higher modes of operation of the antenna. The length 'L' of the patch indicated is calculated using the formula,

$$L = \frac{c}{2f_0\sqrt{\varepsilon_{eff}}} - 0.824h\left[\frac{\varepsilon_{eff}+0.3\left(\frac{w}{h}+0.264\right)}{\varepsilon_{eff}-0.258\left(\frac{w}{h}+0.8\right)}\right] \quad (5)$$

Taking into account the effect of fringing, the total increase in length of the patch denoted by ΔL is given by,

$$\Delta L = 0.5\left(\frac{c_0}{2f_r\sqrt{\varepsilon_{eff}}} - L\right) \quad (6)$$

The resonant frequency is denoted by 'f_r'. The width of the feed line is calculated using the formula,

$$Z_0 = \left(\frac{60}{\sqrt{\varepsilon_{eff}}}\right)\ln\left(\frac{2h}{W}\right) \quad (7)$$

Where Z_0=50Ω is the characteristic impedance of the transmission line.

3. Materials and Methods

3.1. Microstrip Patch

The substrate material of the microstrip patch antenna used for simulation is FR-4, with a dielectric constant of 4.3. The antenna's geometry to be designed with a single patch typically looks as shown in Figure 1 with width 'W' and height 'H' of the substrate. Various methods of feeding the microstrip patch antennas and their arrays depend upon the application and the scenario. Here, the inset feed method is used, which has the advantage of coplanarity between the

antenna and feedline. This produces some capacitance along the input section of the feedline. The various parameters, their symbol and calculated dimensions are shown in Table 2. The calculations and simulations are done separately for uplink and downlink frequencies for a typical n78 5G communication link.

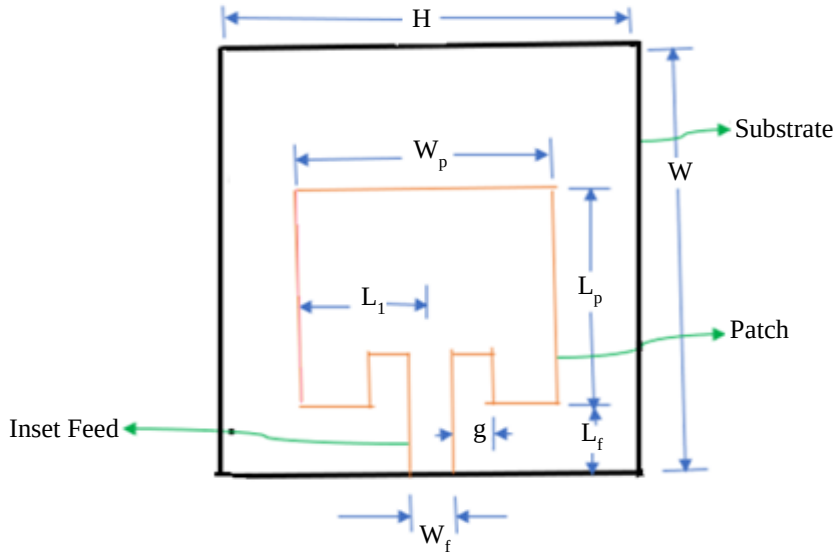

Fig. 1 Geometry of microstrip patch with inset feed

Table 2. Design specifications and dimensions of single patch element

Parameter	Symbol	Uplink	Downlink
Operating Frequency	f_0	3.6 GHz	3.4 GHz
Substrate Height	H	40 mm	42 mm
Substrate Width	W	32 mm	29.5 mm
Patch Length	L_p	20.7 mm	20.5 mm
Patch Width	W_p	32 mm	32 mm
Dielectric Constant	ε_r	4.3	4.3
Feed Line Length	L_f	13 mm	11.5 mm
Feed Line Width	W_f	0.3 mm	0.3 mm
The Gap between Feed Line and Patch	g	14.7 mm	14.95 mm
Feed Inset from Edge	L_1	15 mm	15.25 mm

The single microstrip patch and the array are fed with an inset feed designated with a lumped port at the inset for better impedance matching in the network. The typical impedance to be matched is 50Ω according to Indian standards for a specific microwave transmission line.

The depiction of the patch antenna with dimensions for uplink and downlink frequencies is shown in Figures 2 and 3**,** respectively. The parameter 'g', the gap between the feed line and radiating patch, decides the impedance matching of the network or the designed antenna. This can be adjusted by trial-and-error method for achieving minimal power losses while feeding the antennas or the arrays.

Hence, the values of gap 'g' are varied for uplink and downlink to enable the antenna to resonate at different frequencies. Since 'g' is interconnected with the parameter L_1, which is the length between the feed inset and the edge of the patch, as and when the value of 'g' is varied (increased /decreased), the corresponding value of L_1 must also be changed accordingly as in Table 2.

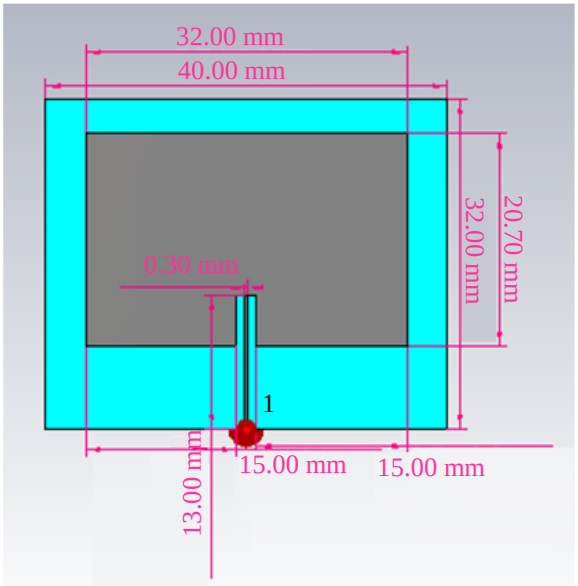

Fig. 2 Design layout and dimensions of patch for uplink

Port 1 at the inset feed is taken as a lumped port, providing better impedance matching at the network. This will also minimize reflections at the port and maximize power transfer to the radiating patch. The calculated dimensions for the patch, substrate and feed line for uplink 3.6 GHz are shown in Table 2. The diagrammatic representation is as in Figure 2.

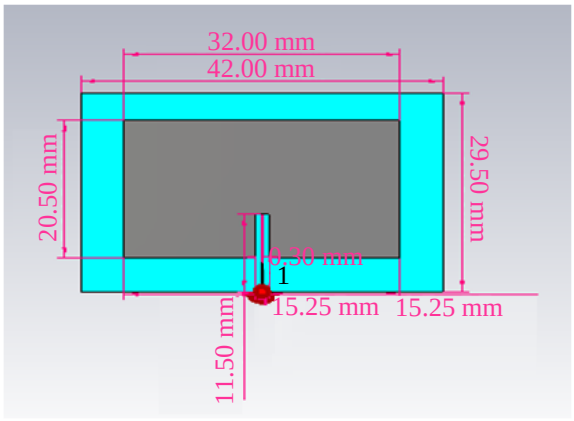

Fig. 3 design layout and dimensions of patch for downlink

The parameters customized for the patch to radiate at a different frequency for downlink (3.4 GHz) are substrate height, substrate width, patch length, feedline length, and the gap between feedline and patch. The calculated dimensions are shown in Table 1. The diagrammatic representation of the same is as shown in Figure 3.

3.2. Microstrip Patch 1x2 Array

The layout and array geometry of a 1x2 array with a 3 dB power divider are shown in Figure 4, with the array's dimensions designed using the equations from (5) to (7). In the design of a 1x2 array, the parameters used for a single patch design with an inset feed are optimized and used to design an array feed network. The impedances are matched to the Indian standard 50Ω transmission line. A 3dB power divider divides the power fed from the lumped port (or the feedline) equally between the two radiating patches.

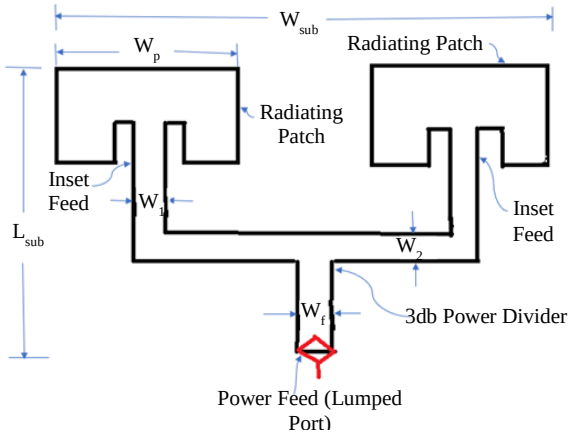

Fig. 4 Geometry of 1x2 array

The design layout and dimensions of the 1x2 array are shown in Figure 5, designed to resonate at 3.67 GHz for uplink.

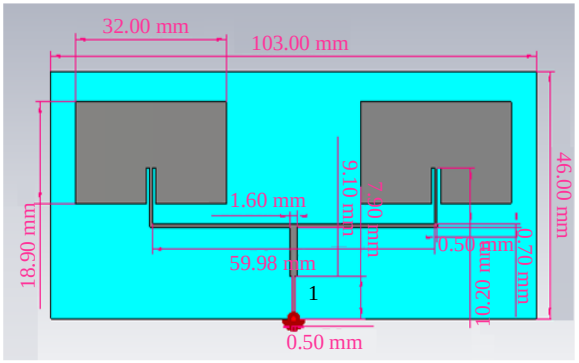

Fig. 5 Design layout and dimensions of 1x2 array for uplink

The substrate used for array design is FR4 with a dielectric constant of 4.3 and is the same as that used for a single microstrip patch. The design layout and dimensions of the 1x2 array for downlink are, as shown in Figure 6, customized to resonate at 3.42 GHz.

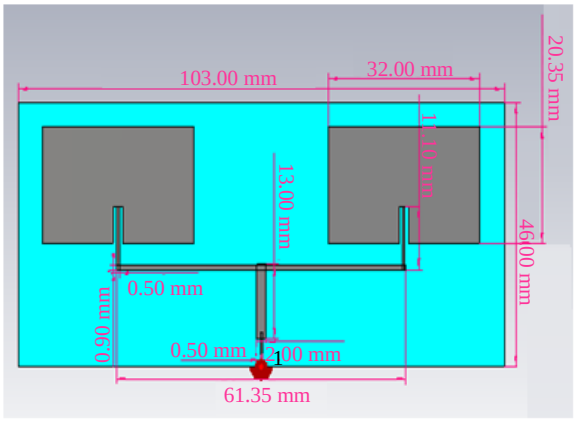

Fig. 6 Design layout and dimensions of 1x2 array for downlink

The dimensions of W_1 and W_2 are changed for the downlink to resonate at 3.4 GHz, as shown in Figure 6. A summary of the design parameters for a 1x2 array for uplink and downlink is given in Table 3.

Table 3. Parameters for 1x2 array

Parameters	Uplink	Downlink
W_{sub}	103 mm	103 mm
L_{sub}	46 mm	46 mm
W_p	32 mm	32 mm
W_1	1.6 mm	0.5 mm
W_2	0.5 mm	0.9 mm
W_f	1.6 mm	0.5 mm

The total length of the substrate, W_{sub}, is kept constant for both uplink and downlink. However, the distance between the power feed (lumped port) and the 3dB power divider, denoted by W_2, is varied so that the array resonates at different frequencies as designed.

4. Results and Discussion

The results obtained by simulation of the primary microstrip patch antenna and 1x2 array are presented in detail with the comparison with designed values in the following sections.

4.1. Uplink Single Patch

Uplink refers to any data, signal, or command frequency transmitted from an earth station to a satellite, aeroplane, or base station. It forms one of the ways of communication in a typical two-way or full duplex communication link.

The resonant frequency is at 3.675GHz, as in Figure 7 (a). It gives a return loss of -28.068dB, good impedance matching of nearly 52Ω and far-field gain of 6.22dB, as shown in Figures 7 (b), (c), (d) and (e), respectively.

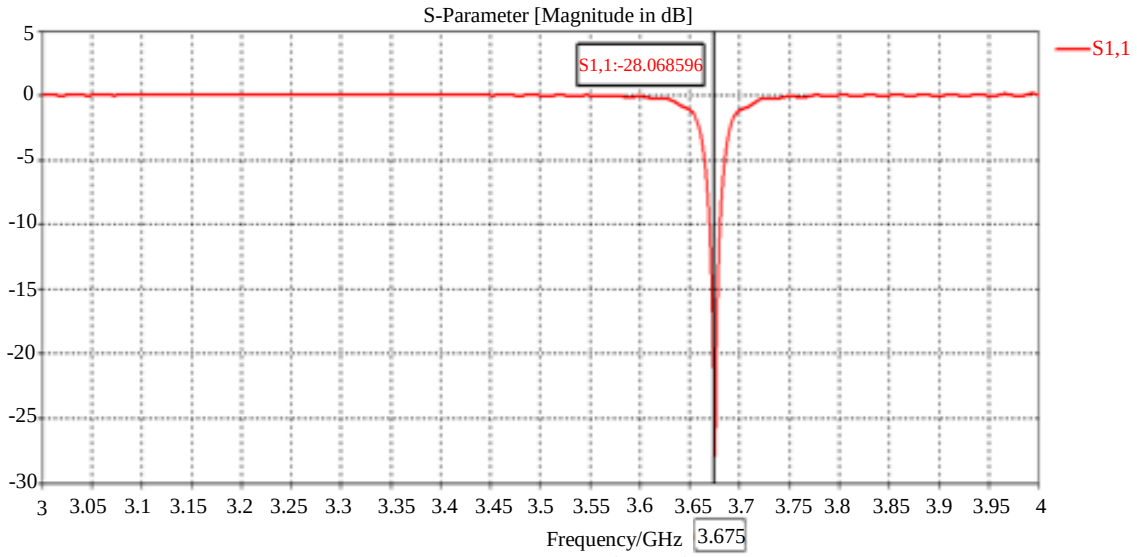

Fig. 7 (a) Antenna BW of patch for uplink

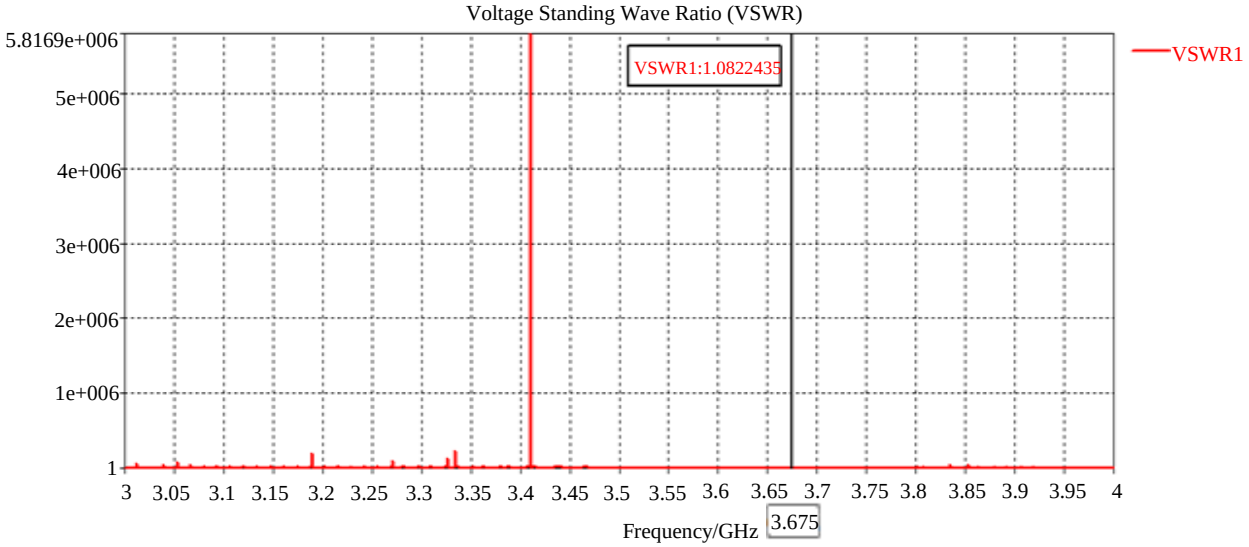

Fig. 7 (b) Return loss of patch for uplink

The patch radiates at 3.675 GHz, excellently matching the designed frequency for uplink with a phenomenal value of S_{11} of -28.068dB, as shown in Figure 7 (a). The single patch has a good impedance match with a VSWR of 1.0842335, as in Figure 7 (b).

The Smith chart plot or the impedance plot of the single patch, as shown in Figure 7 (c), indicates 52.200714Ω, approximately 50Ω; that of a standard microwave transmission line.

The 2D gain pattern of the simple patch, as shown in Figure 7 (d), indicates a maximum gain of 6.22dB with a Side Lobe Level (SLL) of -7.8 dB. Relatively low losses in minor lobes imply that antenna can be employed for commercial and military applications.

The radiation of the patch element is most substantial along the z-direction or azimuthal plane at 6.22dB, as shown in Figure 7 (e) of the 3D radiation plot. The gain will be further increased using an array with constant interelement spacing.

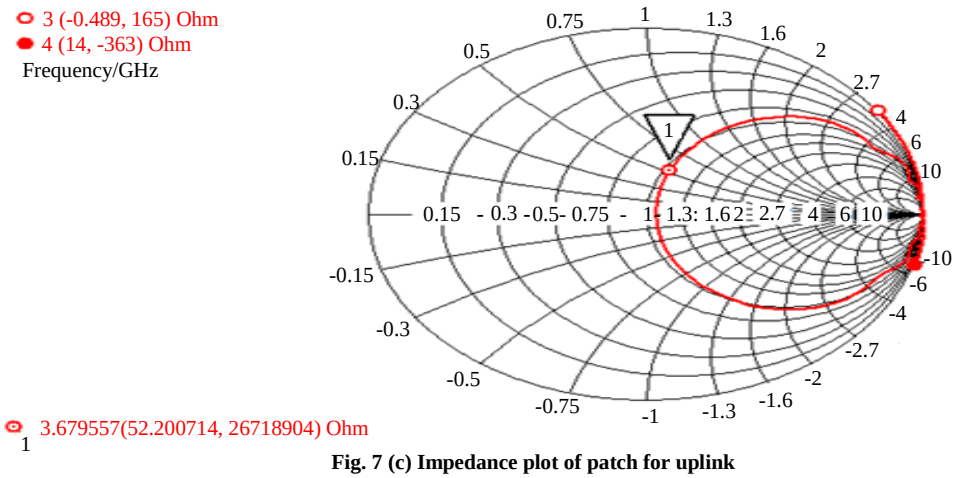

Fig. 7 (c) Impedance plot of patch for uplink

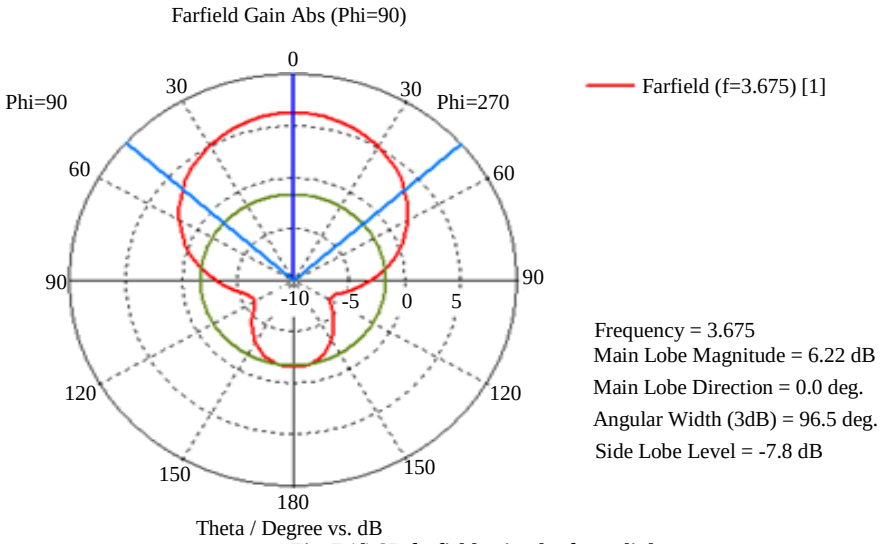

Fig. 7 (d) 2D farfield gain plot for uplink

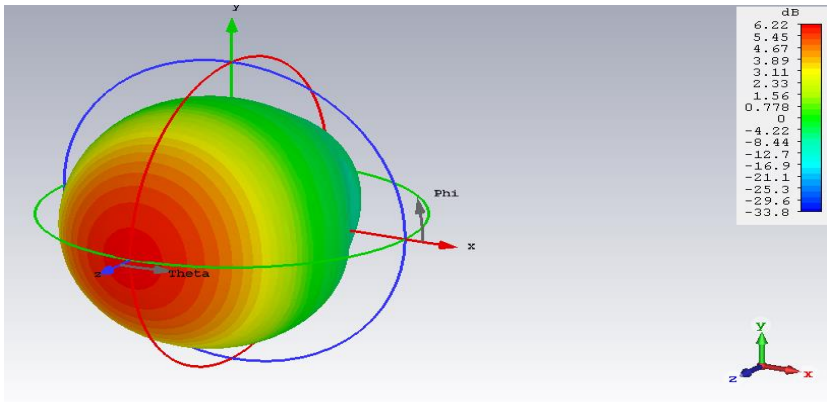

Fig. 7 (e) 3D gain plot of patch for uplink

4.2. Downlink Single Patch

Downlink refers to any data, signal, or command frequency transmitted from a communication satellite, aeroplane, or base station to an earth station or mobile station. It forms the second path or the path to complete the loop in a typical two-way or full duplex communication link. The resonant frequency is at 3.417 GHz, as shown in Figure 8 (a). It gives a return loss of -19.7704dB, fairly good impedance matching of nearly 55Ω and far-field gain of 5.3dB, as shown in Figures 8 (b), (c), (d) and (e), respectively.

The patch for downlink radiates or resonates at 3.417 GHz, excellently matching the 3.4 GHz designed value with the S_{11} value of -19.770441dB as in Figure 8 (a).

The excellent VSWR value of 1.2288546 obtained for downlink, as indicated by Figure 8 (b), gives suitable impedance matching high performance with minimal antenna mismatch-related losses.

The impedance plot of Figure 8 (c) indicates that impedance is matched at 55.208901Ω at 1.6 VSWR. This slightly differs from the ideal values, indicating the need for matching networks and optimization techniques.

The 2D radiation pattern of the downlink, as shown in Figure 8 (d), offers a gain of 5.3dB with an SLL of -8.1 dB. The perfect end-fire pattern of the antenna is revealed in the fact that the main lobe is oriented at 0°, which is the axis of the array. The radiation is maximum along the z-axis or azimuthal plane for the down-link patch with a gain of 5.33dB, as shown in Figure 8 (e). The radiation pattern is somewhat circular, nearing isotropic radiation. The array further enhances this gain, as explained in the following sections.

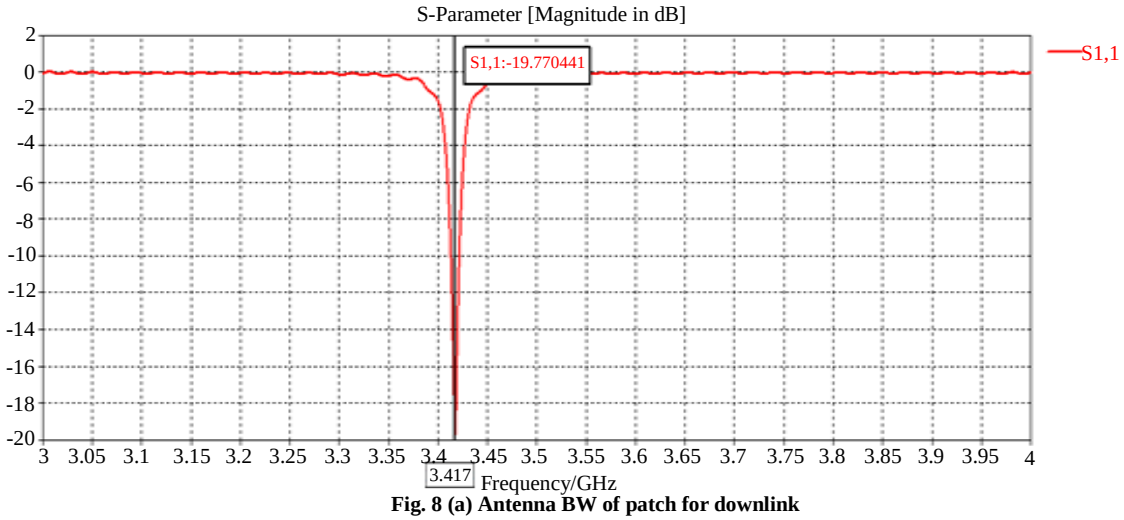

Fig. 8 (a) Antenna BW of patch for downlink

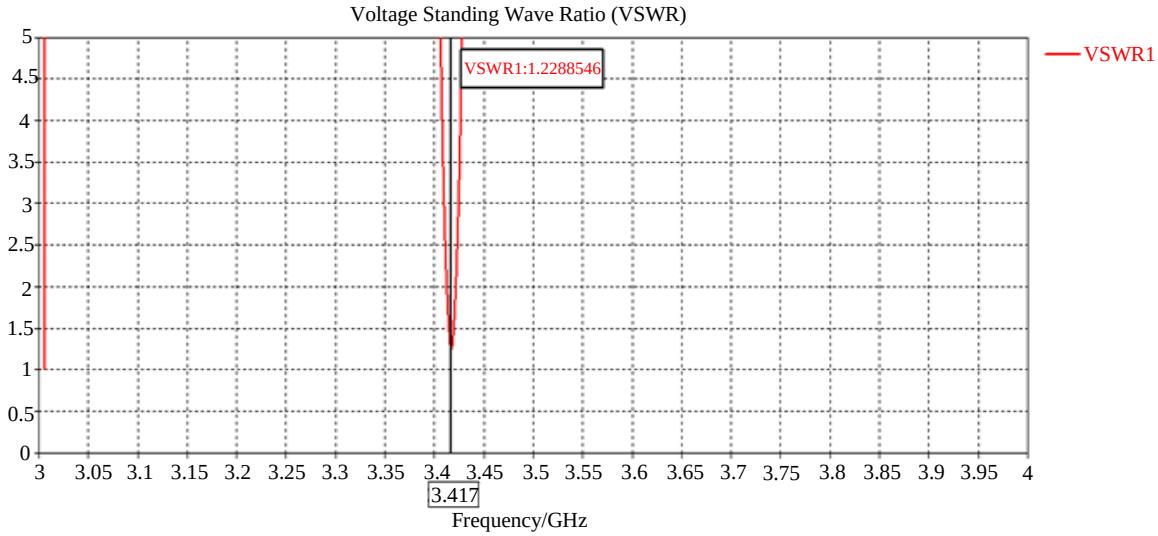

Fig. 8 (b) Return loss of patch for downlink

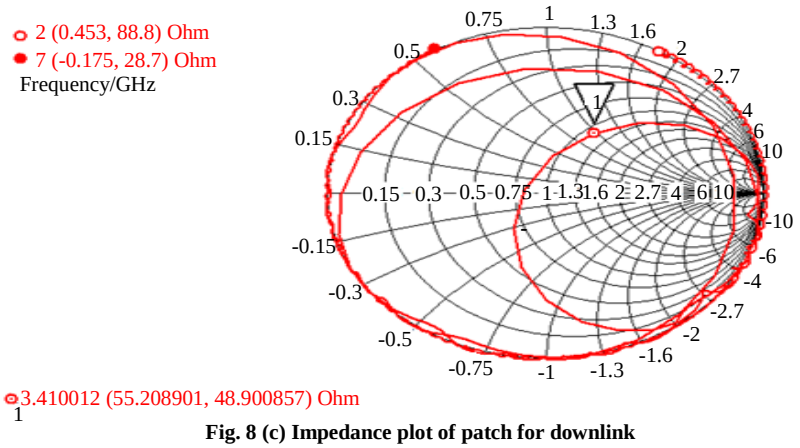

Fig. 8 (c) Impedance plot of patch for downlink

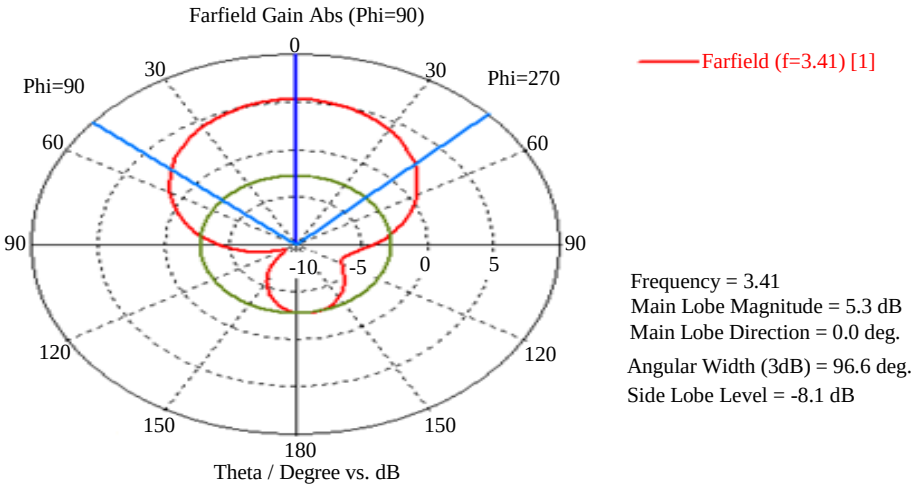

Fig. 8 (d) 2D farfield gain plot for downlink

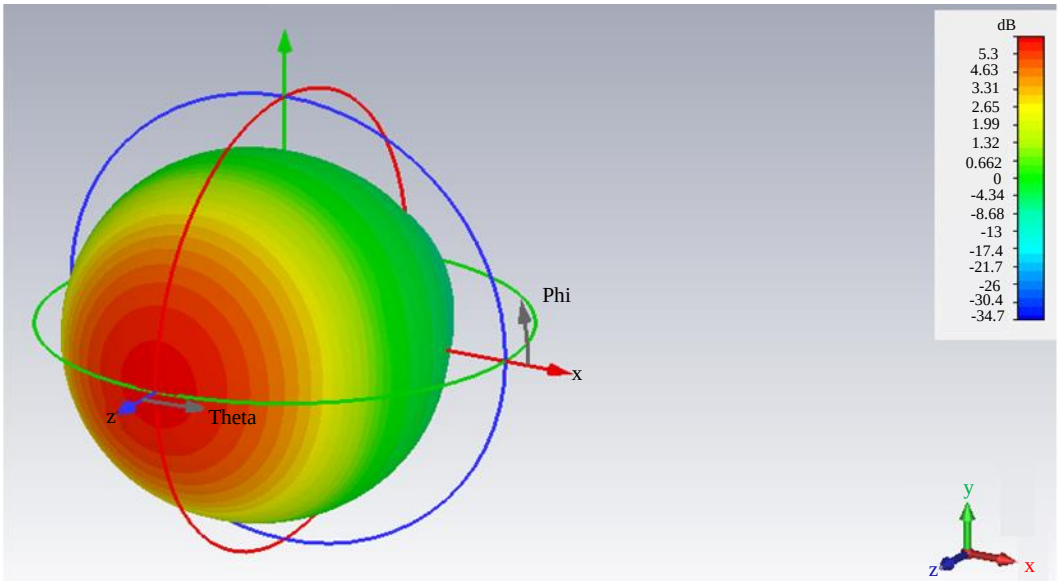

Fig. 8 (e) 3D gain plot of patch for downlink

4.3. x2 Array Uplink

The resonant frequency for uplink is 3.679GHz with a return loss of -25.07889dB, with precise VSWR and impedance matching as shown in Figure 9 (a), (b) and (c), respectively. The overall gain of the antenna has improved to 10.1dB, as in Figures 9 (d) and (e) from 6.22dB for a single patch.

This shows an increased gain of 3.88dB using an inset-fed array compared to a single microstrip patch. The gain can be further improved by adding more array elements (increasing the size of the array) and changing the feeding techniques of the array.

The 1x2 array for uplink resonates at 3.679 GHz, which matches the designed value shown in Figure 9 (a) with a return loss of -25.07889dB. This indicates efficient power transfer between the array elements.

The good VSWR value of 1.1180286 indicated in Figure 9 (b) is lesser than that obtained for a single patch and signifies better impedance matching, optimal antenna performance, efficient power transfer and minimal losses.

The impedance plot of Figure 9 (c) indicates that matching networks are not required because the matched impedance is at 51.987169 Ω at 1.1 VSWR matches the ideal values.

The 2D radiation plot of the array shows the phenomenal gain of 10.1dB at the resonant frequency, as shown in Figure 9 (d), with a reduced SLL of -13.1 dB. The array is the end-fire type with a minimal tilt of 10° from the axis of the array.

The 3D radiation pattern, as shown in Figure 9 (e), offers a maximum gain of 10.1 dB along the y-axis or the elevation plane, indicating a broadside type of operation.

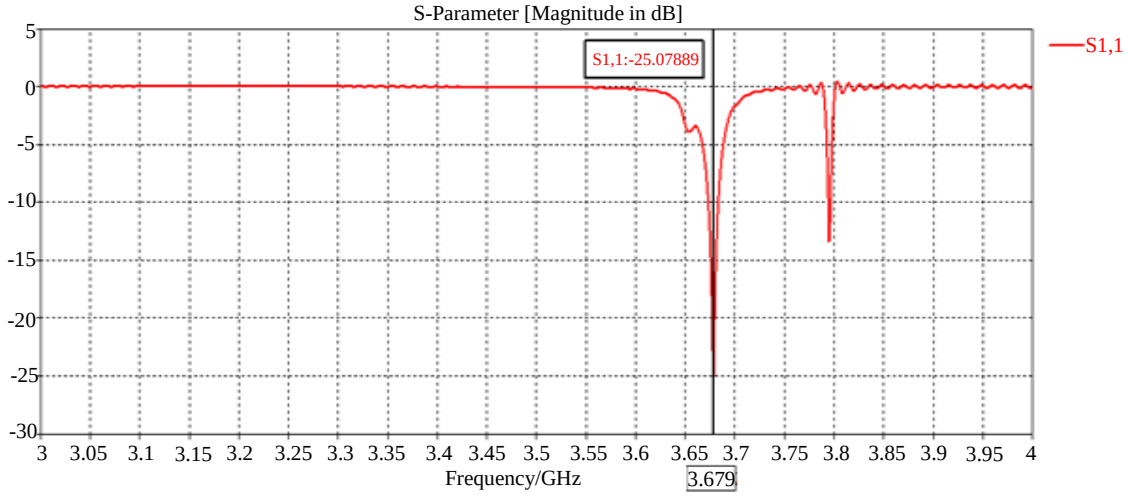

Fig. 9 (a) Antenna BW plot of 1x2 array uplink

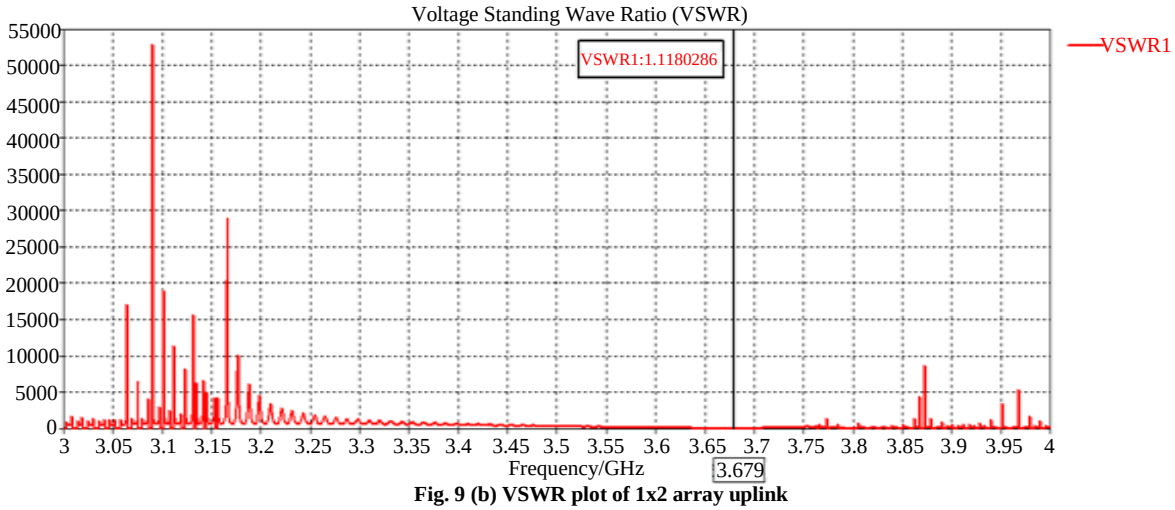

Fig. 9 (b) VSWR plot of 1x2 array uplink

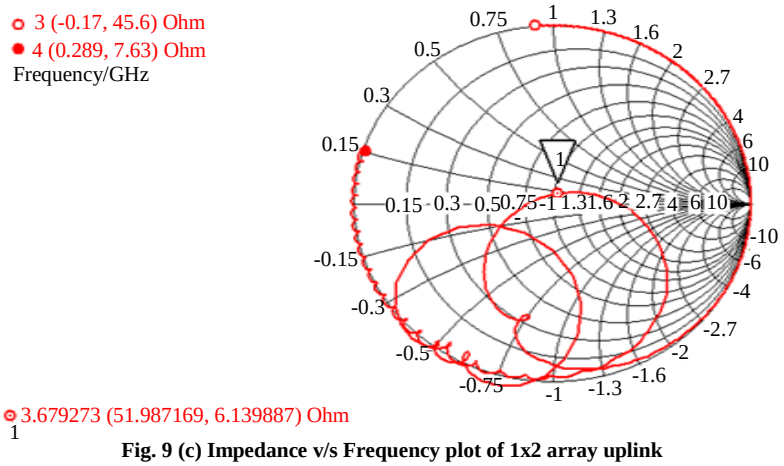

Fig. 9 (c) Impedance v/s Frequency plot of 1x2 array uplink

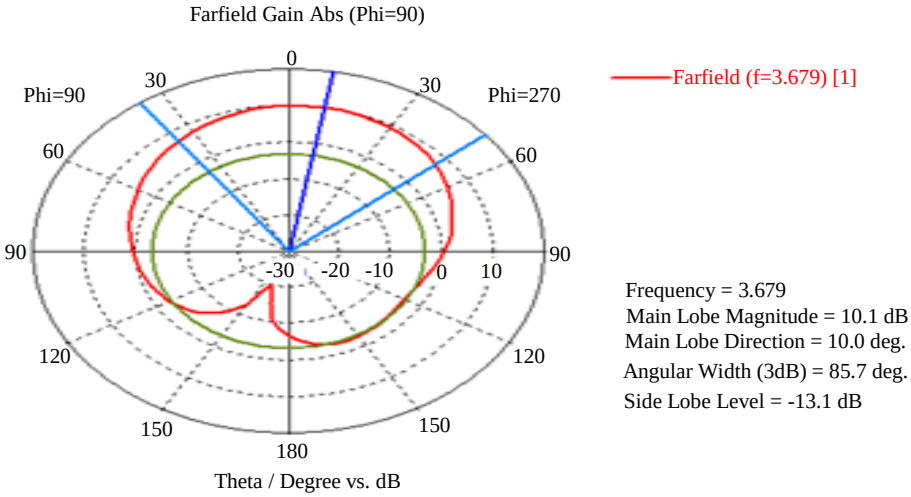

Fig. 9 (d) 2D farfield gain plot of 1x2 array uplink

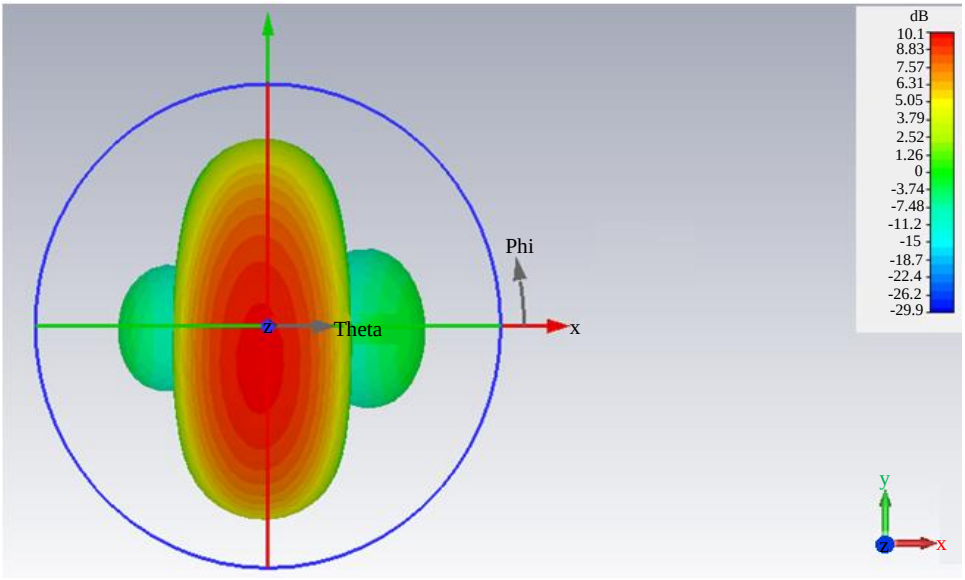

Fig. 9 (e) 3D gain plot of 1x2 array uplink

4.4. 1x2 Array Downlink

The resonant frequency for downlink is 3.426GHz with a return loss of -28.103712dB, with precise VSWR and impedance matching as shown in Figure 10 (a), (b) and (c), respectively. The overall gain of the antenna has improved to 9.31dB, as in Figures 10 (d) and (e) from 5.3dB for a single patch. This shows an increased gain of 4.01dB using an inset-fed array compared to a single microstrip patch. The gain can be further improved by adding more array elements (increasing the size of the array) and changing the feeding techniques of the array.

The 1x2 array for downlink resonates at 3.426 GHz with a good return loss of -28.103712 dB, as shown in Figure 10(a). The pattern shows a sharp cut-off at the resonant frequency of 3.426 GHz, facilitating communication applications for point-to-point or LOS (Line of Sight). This also proves extremely helpful in defence and military applications where only the intended end user or destination is supposed to receive the information from the transmitter.

The VSWR value of 1.0818981 obtained for the downlink, as shown in Figure 10 (b), is very close to 1, the ideal value. This indicates the best antenna performance efficiency with antenna elements radiating and receiving powers with no reflected waves. This also shows less mutual coupling effects between the array elements.

The impedance plot of Figure 10 (c) for the downlink array indicates that best matching occurs at 49.471035Ω at 1.1 VSWR, eliminating the need for impedance matching networks and consequently minimizing losses in the network.

The 2D radiation plot of the downlink array shows the phenomenal gain of 9.31dB at the resonant frequency, as shown in Figure 10 (d), with a reduced SLL of -12.7 dB. The array shows an increased gain of around 4dB compared to the single patch. The array is the end-fire type with a minimal tilt of 5° from the axis of the array.

The 3D radiation pattern, as shown in Figure 10 (e), offers a maximum gain of 9.31 dB along the y-axis or the elevation plane, indicating a broadside type of operation. The comparison of various designed parameters and the obtained values after simulation have been tabulated in Table 4. The inference that can be drawn from the table is the array elements contribute to better gain, better impedance matching and nearly ideal VSWR values than the single radiating element.

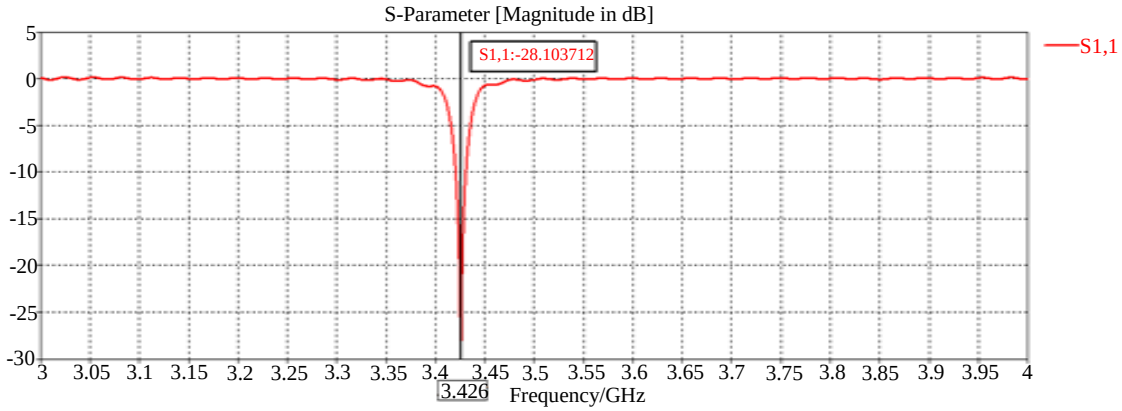

Fig. 10 (a) Antenna BW plot of 1x2 array downlink

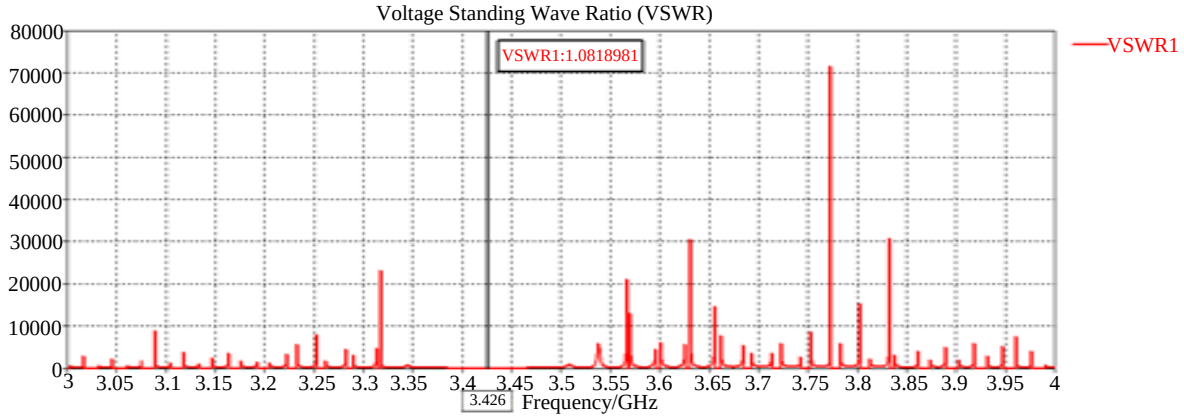

Fig. 10 (b) VSWR plot of 1x2 array downlink

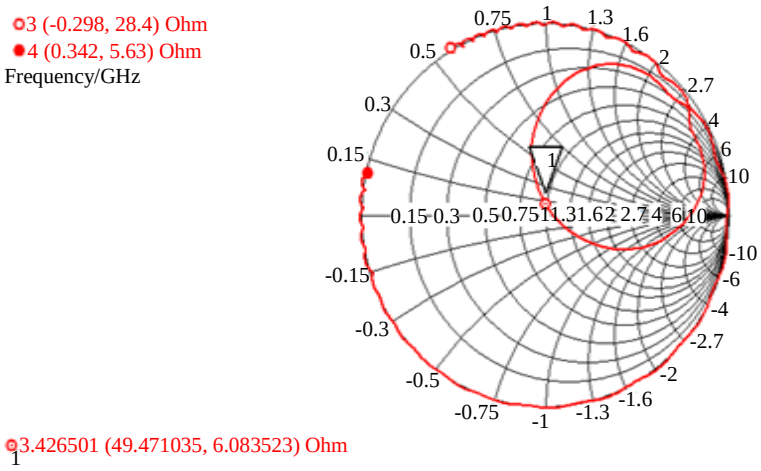

Fig. 10 (c) Impedance v/s Frequency plot of 1x2 array downlink

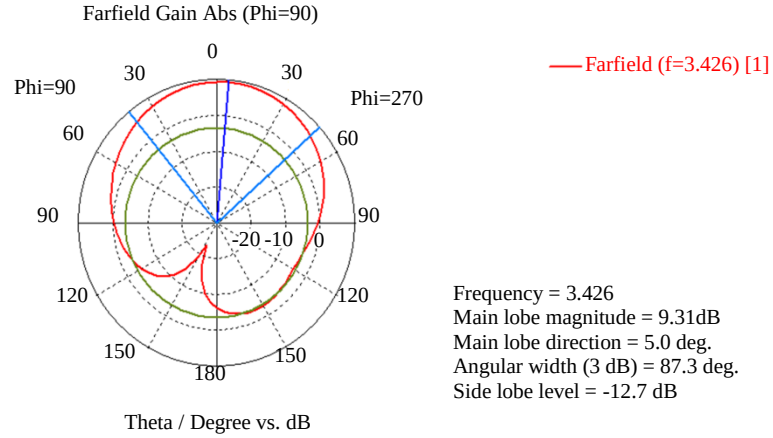

Fig. 10 (d) 2D Farfield gain plot of 1x2 array downlink

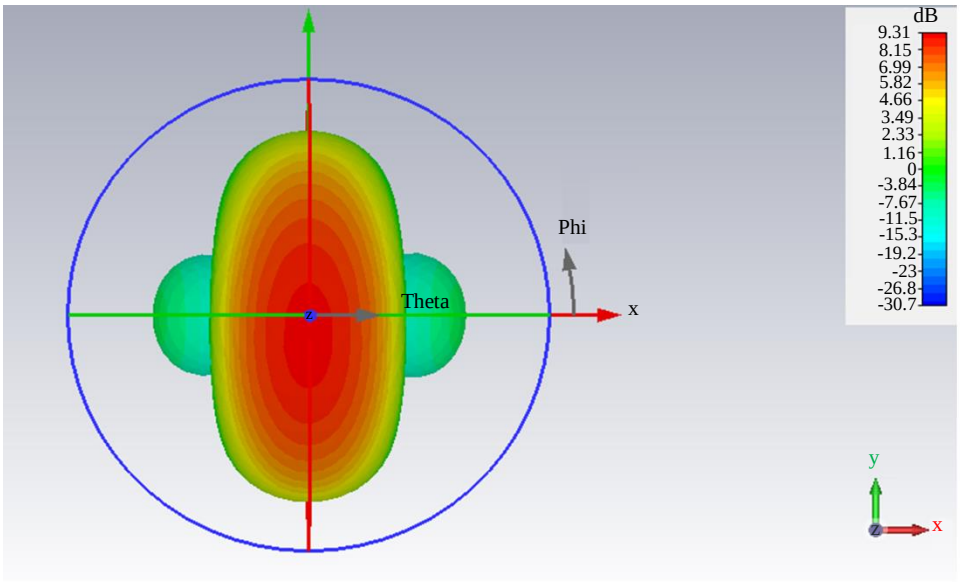

Fig. 10 (e) 3D Gain plot of 1x2 array downlink

Table 4. Comparison of designed and simulated parameters for single element and 1x2 array

Parameter	Single Patch		1x2 array	
	Uplink	Downlink	Uplink	Downlink
Resonant Frequency (GHz)	3.675	3.417	3.679	3.426
VSWR	1.0822	1.2288	1.1180	1.0818
Impedance Matching (Ω)	52.2007	55.2089	51.9871	49.4710
Return Loss (dB)	-28.0685	-19.7704	-25.0788	-28.1037
Gain (dB)	6.22	5.3	10.1	9.31

5. Conclusion

This research presents a novel approach to designing and simulating conformal antennas for 5G communication bands with two antennas for uplink and downlink in the n78 band. The results for a single microstrip patch element and a 1x2 array are compared. The power feeding technique used for both cases is inset feed, which provides a planar structure suitable for apt impedance matching between the radiating patch and the feedline. It is also observed that the array elements exhibit an increased gain and more performance efficiency than that of a single component. The growth has increased by approximately 4dB in the array system compared to the single-element system.

Further increase in gain and directivity can be obtained by designing a 1x4 array or any other higher-order array with more array elements. Impedance matching of nearly 50Ω is achieved in a 1x2 collection rather than a single radiating patch. Thus, the arrays are designed for avionics, navigation and air traffic control applications. The design is done in the world's most popular mid-range frequency band of 5G, which provides data speeds up to 1 Gbps.

References

[1] Mamta Agiwal, Abhishek Roy, and Navrati Saxena, "Next Generation 5G Wireless Networks: A Comprehensive Survey," *IEEE Communications Surveys and Tutorials*, vol. 18, no. 3, pp. 1617-1655, 2016. [CrossRef] [Google Scholar] [Publisher Link]

[2] Weijia Wang et al., "High-Performance Printable 2.4 GHz Graphene-Based Antenna Using Water-Transferring Technology," *Science and Technology of Advanced Materials*, vol. 20, no. 1, pp. 870-875, 2019. [CrossRef] [Google Scholar] [Publisher Link]

[3] Sumit Kumar et al., "Fifth Generation Antennas: A Comprehensive Review of Design and Performance Enhancement Techniques," *IEEE Access*, vol. 8, pp. 163568-163593, 2020. [CrossRef] [Google Scholar] [Publisher Link]

[4] Rongguo Song et al., "Wideband and Low Sidelobe Graphene Antenna Array for 5G Applications," *Science Bulletin*, vol. 66, no. 2, pp. 103-106, 2020. [CrossRef] [Google Scholar] [Publisher Link]

[5] Xinyao Zhou et al., "Graphene Printed Flexible and Conformal Array Antenna on Paper Substrate for 5.8 GHz Wireless Communications," *2020 14th European Conference on Antennas and Propagation (EuCAP)*, pp. 1-4, 2020. [CrossRef] [Google Scholar] [Publisher Link]

[6] Hao-Ran Zu et al., "Circularly Polarized Wearable Antenna with Low Profile and Low Specific Absorption Rate Using Highly Conductive Graphene Film," *EEE Antennas and Wireless Propagation Letters*, vol. 19, no. 12, pp. 2354-2358, 2020. [CrossRef] [Google Scholar] [Publisher Link]

[7] Wonbin Hong, "Solving the 5G Mobile Antenna Puzzle: Assessing Future Directions for the 5G Mobile Antenna Paradigm Shift," *IEEE Microwave Magazine*, vol. 18, no. 7, pp. 86-102, 2017. [CrossRef] [Google Scholar] [Publisher Link]

[8] Wei Hong et al., "Multibeam Antenna Technologies for 5G Wireless Communications," *IEEE Transactions on Antennas and Propagation*, vol. 65, no. 12, pp. 6231-6249, 2017. [CrossRef] [Google Scholar] [Publisher Link]

[9] Syeda Fizzah Jilani et al., "Millimeter-Wave Liquid Crystal Polymer Based Conformal Antenna Array for 5G Applications," *IEEE Antennas and Wireless Propagation Letters*, vol. 18, no. 1, pp. 84-88, 2019. [CrossRef] [Google Scholar] [Publisher Link]

[10] Chun-Xu Mao et al., "Planar Sub-Millimeter-Wave Array Antenna with Enhanced Gain and Reduced Sidelobes for 5G Broadcast Applications," *IEEE Transactions on Antennas and Propagation*, vol. 67, no. 1, pp. 160-168, 2019. [CrossRef] [Google Scholar] [Publisher Link]

[11] Lars Josefsson, and Patrik Persson, *Conformal Array Antenna Theory and Design*, IEEE Press Series on Electromagnetic Wave Theory, John Wiley and Sons, pp. 1-83, 2006. [Google Scholar] [Publisher Link]

[12] Wael Ali et al., "Planar Dual-Band 27/39 GHz Millimeter-Wave MIMO Antenna for 5G Applications," *Microsystem Technologies*, vol. 27, pp. 283-292, 2021. [CrossRef] [Google Scholar] [Publisher Link]

[13] Oluseun Oyeleke Wikiman et al., "PIFA Antenna Design for MmWave Body Centric 5G Communication Applications," SSRG *International Journal of Electronics and Communication Engineering*, vol. 6, no. 4, pp. 6-10, 2019. [CrossRef] [Google Scholar] [Publisher Link]

[14] Thomas E. Morton, and Krishna M. Pasala, "Pattern Synthesis of Conformal Arrays for Airborne Vehicles," *2004 IEEE Aerospace Conference Proceedings*, vol. 2, pp. 1030-1039, 2004. [CrossRef] [Google Scholar] [Publisher Link]

[15] Jiazhi Dong et al., "A Research on Airborne Conformal Array with High Gain and Low SLL," *2014 International Conference on Computational Intelligence and Communication Networks*, pp. 334-338, 2014. [CrossRef] [Google Scholar] [Publisher Link]

[16] Yeqin Huang, and Shieh T. Hsieh, "Radiation of Conformal Slot Arrays on Perfectly Conducting Super-Spheroid," *2005 IEEE International Symposium on Microwave, Antenna, Propagation and EMC Technologies for Wireless Communications*, vol. 1, pp. 601-604, 2005. [CrossRef] [Google Scholar] [Publisher Link]

[17] L. Zou, J. Lasenby, and Z. He, "Beamforming with Distortion Less Co-Polarization for Conformal Arrays Based on Geometric Algebra," *IET Radar, Sonar and Navigation*, vol. 5, no. 8, pp. 842-853, 2011. [CrossRef] [Google Scholar] [Publisher Link]

[18] K.M. Tsui, and S.C. Chan, "Pattern Synthesis of Narrowband Conformal Arrays Using Iterative Second-Order Cone Programming," *IEEE Transactions on Antennas and Propagation*, vol. 58, no. 6, pp. 1959-1970, 2010. [CrossRef] [Google Scholar] [Publisher Link]

[19] Yan-Ying Bai et al., "A Hybrid IWO/PSO Algorithm for Pattern Synthesis of Conformal Phased Arrays," *IEEE Transactions on Antennas and Propagation*, vol. 61, no. 4, pp. 2382-2332, 2013. [CrossRef] [Google Scholar] [Publisher Link]

[20] Massimiliano Comisso, and Roberto Vescovo, "3D Power Synthesis with Reduction of Near-Field and Dynamic Range Ratio for Conformal Antenna Arrays," *IEEE Transactions on Antennas and Propagation*, vol. 59, no. 4, pp. 1164-1174, 2011. [CrossRef] [Google Scholar] [Publisher Link]

[21] Srabonty Soily, Rezaul Karim Mazumder, and Khaleda Ali, "Design and Simulation of Two Conformal Arrays with Dual Patch and Quadruple Patch Antenna Elements," *2015 IEEE Conference on Antenna Measurements and Applications (CAMA)*, pp. 1-3, 2015. [CrossRef] [Google Scholar] [Publisher Link]

[22] M. Comisso, and Roberto Vescovo, "Fast 3D Pattern Synthesis for Conformal Antenna Arrays with Cross-Polarization Reduction," *2010 IEEE Antennas and Propagation Society International Symposium*, pp. 1-4, 2010. [CrossRef] [Google Scholar] [Publisher Link]

[23] Meysam Rasekh, and Saeid R. Seydnejad, "Design of an Adaptive Wideband Beamforming Algorithm for Conformal Arrays," *IEEE Communications Letters*, vol. 18, no. 11, pp. 1955-1958, 2014 [CrossRef] [Google Scholar] [Publisher Link]

[24] K. Woelders, and J. Granholm, "Cross-Polarization and Sidelobe Suppression in Dual Linear Polarization Antenna Arrays," *IEEE Transactions on Antennas and Propagation*, vol. 45, no. 12, pp. 1727-1740, 1997. [CrossRef] [Google Scholar] [Publisher Link]

[25] Harmen Schippers et al., "Conformal Phased Array with Beam Forming for Airborne Satellite Communication," *2008 International ITG Workshop on Smart Antennas*, pp. 334-350, 2008. [CrossRef] [Google Scholar] [Publisher Link]

[26] Peter Knott, "Design of a Triple Patch Antenna Element for Double Curved Conformal Antenna Arrays," *2006 First European Conference on Antennas and Propagation*, pp. 1-4, 2006. [CrossRef] [Google Scholar] [Publisher Link]

[27] Ziheng Ding et al., "High Aperture Efficiency Arced Conformal Array with Phasor Beam Steering Antenna," *IEEE Transactions on Antennas and Propagation*, vol. 71, no. 1, pp. 596-605, 2022. [CrossRef] [Google Scholar] [Publisher Link]

[28] Fujun Xu et al., "Performance and Impact Damage of a Three Dimensionally Integrated Microstrip Feeding Antenna Structure," *Composite Structures*, vol. 93, no. 1, pp. 193-197, 2010. [CrossRef] [Google Scholar] [Publisher Link]

[29] Lan Yao et al., "Fabrication and Impact Performance of Three-Dimensionally Integrated Microstrip Antennas with Microstrip and Coaxial Feeding," *Smart Materials and Structures*, vol. 18, no. 9, 2009. [CrossRef] [Google Scholar] [Publisher Link]

[30] Brajlata Chauhan et al., "Cylindrical Conformal Antenna Arrays Theory for Military Aircraft Antenna," *2020 IEEE International Conference on Computing, Power and Communication Technologies (GUCON)*, pp. 77-82, 2020. [CrossRef] [Google Scholar] [Publisher Link]

[31] Bahare Mohamadzade et al., "Recent Developments and State of the Art in Flexible and Conformal Reconfigurable Antennas," *Electronics*, vol. 9, no. 9, pp. 1-26, 2020. [CrossRef] [Google Scholar] [Publisher Link]

[32] Garima D. Bhatnagar et al., "Design of Broadband Circular Patch Microstrip Antenna with Diamond Shape Slot," *Indian Journal of Radio and Space Physics*, vol. 40, pp. 275-281, 2011. [Google Scholar] [Publisher Link]

[33] Neng-Wu Liu et al., "A Low-Profile Aperture-Coupled Microstrip Antenna with Enhanced Bandwidth Under Dual Resonance," *IEEE Transactions on Antennas and Propagation*, vol. 65, no. 3, pp. 1055-1062, 2017. [CrossRef] [Google Scholar] [Publisher Link]

[34] Ling Sun et al., "Two-Port Pattern Diversity Antenna for 3G and 4G MIMO Indoor Applications," *IEEE Antennas and Wireless Propagation Letters*, vol. 13, pp. 1573-1576, 2014. [CrossRef] [Google Scholar] [Publisher Link]

[35] Wei Lin, Richard W. Ziolkowski, and Hang Wong, "Pattern Reconfigurable Techniques for LP and CP Antennas with the Broadside And Conical Beams," *12th European Conference on Antennas and Propagation (EuCAP 2018)*, pp. 1-4, 2018. [CrossRef] [Google Scholar] [Publisher Link]